Scattering Coefficients of an Inductive Strip in a Finline: Theory and Experiment

JEFFREY B. KNORR, SENIOR MEMBER, IEEE, AND JOHN C. DEAL

Abstract—**This paper describes the application of the spectral-domain method to the computation of the scattering coefficients of an inductive strip in a millimeter-wave finline. Measured scattering data are compared with numerical data to establish the accuracy of the results. The predicted and measured responses of several finline resonators are also compared.**

I. Introduction

THE USE OF finline as a transmission structure for millimeter-wave integrated circuits was first proposed by Meier in 1974 [1]. Since that time, the practical utility of finline has been discussed in the literature by numerous authors and various theoretical analyses have been published. Recently, a comprehensive review, "The status of printed millimeter-wave *E*-plane circuits," was published by Solbach [2]. That review contains an exhaustive list of references to the existing literature so that effort will not be duplicated here. Finline has become established as a viable structure and, therefore, analyses contributing to its effective utilization are of widespread interest.

The spectral-domain method has proven to be a particularly versatile technique for analyzing the behavior of planar transmission lines in general and finline in particular. Knorr and Shayda have applied this method to determine the transmission characteristics of finline [3] and Jansen [4] and Knorr [5] have used it to investigate the end effect in a shorted finline. The natural extension of the spectral-domain technique to various discontinuity problems has been pointed out by Knorr [5] and by Koster and Jansen [6], [7].

One discontinuity of considerable practical importance is the inductive strip in finline. It is used to construct simple resonators as well as more complicated multiresonator filters. The geometry for an inductive strip is illustrated in Fig. 1, and a cross-sectional view of the finline in which the strip resides is shown in Fig. 2. The electric field in the plane containing the fins is predominantly in the x-direction. A wave incident on the strip induces a current on the strip and the associated stored magnetic energy of the evanescent field gives the strip its inductive property. If the strip is very long, the field decays with distance and the strip behaves like a shorting septum [5]. If the strip is sufficiently short, the incident wave is partially backscattered and partially forward scattered. The scattering coefficients s_{11} and s_{21} are functions of strip width, fin separation, dielectric constant, and shield size. Theoretically, the problem may be solved by computing the odd- and even-mode resonant lengths of finline cavities which are end coupled by the strip. These lengths are then used to compute the complex scattering coefficients of the strip at the specified frequency.

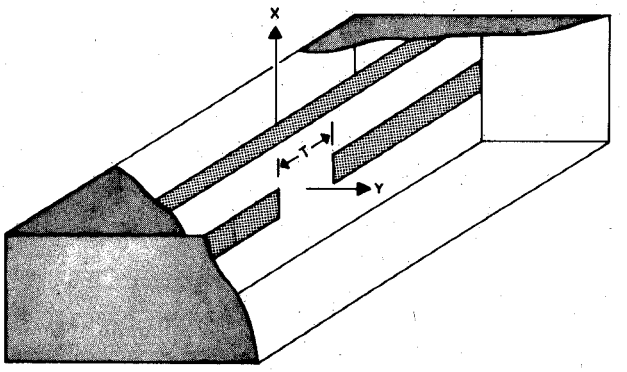

Fig. 1. View of finline inductive strip of axial length T centered in a finline cavity.

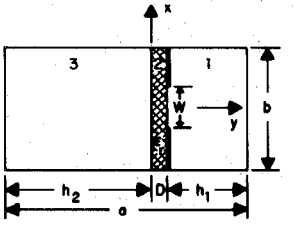

Fig. 2. Cross-sectional view of a finline.

The purpose of this paper is to present the results of both theoretical and experimental investigations of an inductive strip in a unilateral finline. The problem is treated theoretically by applying the spectral-domain method to finline resonators which are end-coupled by a thin, lossless strip. This permits the scattering matrix of the strip to be computed. Experimentally, the strips were investigated in two ways. First, the scattering coefficients for various strips were measured directly. When the strip resides on a dielectric substrate, however, direct measurement of scattering coefficients presents serious practical difficulties since the reference planes for the measurements cannot be easily established. Thus, a second method, measurement of resonator response, was also employed. Two identical strips were used to form a resonator, and the strip scattering

Manuscript received February 20, 1985; revised May 14, 1985.

J. B. Knorr is with the Department of Electrical and Computer Engineering, Naval Postgraduate School, Monterey, CA 93943.

J. C. Deal is with the Department of Electrical Engineering, U.S. Military Academy, West Point, NY 10996.

0018-9480/85/1000-1011$01.00 ©1985 IEEE

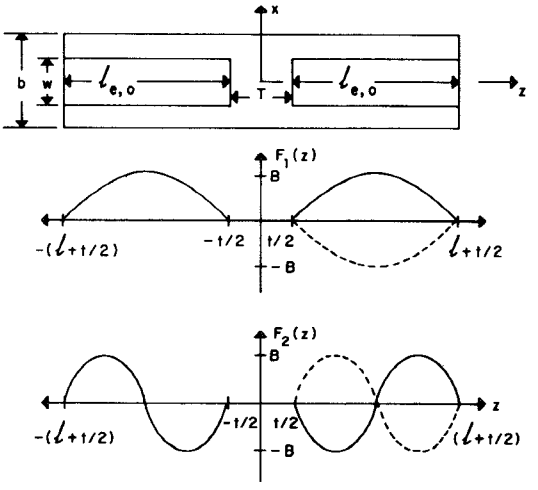

Fig. 3. Coupled finline cavities and basis functions used to expand the even- (solid) and odd- (dashed) mode electric field.

coefficients were extracted from the resonator response. Excellent agreement between numerical and experimental data is demonstrated, thereby establishing the validity of the computational results. Section II of this paper describes the theoretical and experimental methods, and Section III contains the numerical and experimental results. Conclusions appear in Section IV.

II. Theoretical and Experimental Methods

A. Theoretical Method

The spectral-domain solution of the finline cavity problem proceeds as described by Knorr [5]. The particular configuration of interest here, end-coupled resonators, is accommodated by proper choice of modes and a basis set with which the fields of the modes can be expanded. The z-component of the electric field between the fins is assumed to be negligibly small. The geometric structure of the coupled cavities and field distributions of the selected basis functions for the z-dependence of the x-directed electric field e_x^z for both odd and even modes are described in Fig. 3. The end walls are perfect shorts, and the inductive discontinuity is in the center of the structure. The solid curve in Fig. 3 represents the field distribution of the even mode and the dashed curve represents that of the odd mode.

The electric field between the fins may be expanded in the basis set depicted in Fig. 3 as

$$e_x(x,z) = A \sum_{q=1}^{Q} B_q F_q(z), \qquad (|x| < W/2,\ t/2 \leq |z| \leq l + t/2) \quad (1)$$

where the $F_q(z)$ are defined as

$$F_q(z) = \begin{cases} \sin(q\pi/l)[z+(l+t)/2] & (z<0, q \text{ even}) \\ \pm\sin(q\pi/l)[z-(l+t)/2] & (z>0, q \text{ even}) \\ \cos(q\pi/l)[z+(l+t)/2] & (z<0, q \text{ odd}) \\ \pm\cos(q\pi/l)[z-(l+t)/2] & (z>0, q \text{ odd}) \end{cases} \quad (2)$$

For the sine function, plus (+) applies for the odd mode and minus (−) for the even mode, while for the cosine function, plus (+) applies for the even mode and minus (−) for the odd mode.

In the transform domain,

$$F[e_x(x,z)] = E_x^x(\alpha_n) \sum_{q=1}^{Q} B_q E_{xq}^2(\xi_k) \quad (3)$$

where α_n and ξ_k are the x and z transform variables, respectively, as defined by [5, eqs. (4) and (5)]. For q even

$$E_{xq}^{zs}(\xi_k) = \begin{cases} (-1)^q (q\pi l_e/2) \dfrac{\sin\theta}{\theta^2 - \left(\frac{q\pi}{2}\right)^2} 2\sin\xi_k\left(\frac{l_e+t}{2}\right) & \text{(even mode)} \\ (-1)^q (q\pi l_o/2) \dfrac{\sin\theta}{\theta^2 - \left(\frac{q\pi}{2}\right)^2} 2j\cos\xi_k\left(\frac{l_o+t}{2}\right) & \text{(odd mode)} \end{cases} \quad (4a)$$

and for q odd

$$E_{xq}^{zc}(\xi_k) = \begin{cases} (-1)^q (q\pi l_e/2) \dfrac{\cos\theta}{\theta^2 - \left(\frac{q\pi}{2}\right)^2} 2\cos\xi_k\left(\frac{l_e+t}{2}\right) & \text{(even mode)} \\ (-1)^q (q\pi l_o/2) \dfrac{\cos\theta}{\theta^2 - \left(\frac{q\pi}{2}\right)^2} 2j\sin\xi_k\left(\frac{l_o+t}{2}\right) & \text{(odd mode)} \end{cases} \quad (4b)$$

where $\theta = (\xi_k l)/2$. Using Galerkin's Method with the inner product defined as given in [5], we now obtain

$$\langle G_{11} E_x, E_x \rangle = 0 \quad (5)$$

where $E_z = 0$ is assumed and where G_{11} is the Fourier transformed dyadic Green's function component. Assuming $E_x = E_x^x E_x^z$ yields

$$\left[\langle \{E_x^x(\alpha_n)\}^2 G_{11} E_{xi}^z(\xi_k), E_{xj}^z(\xi_k)\rangle\right][B_j] = 0 \quad (6)$$

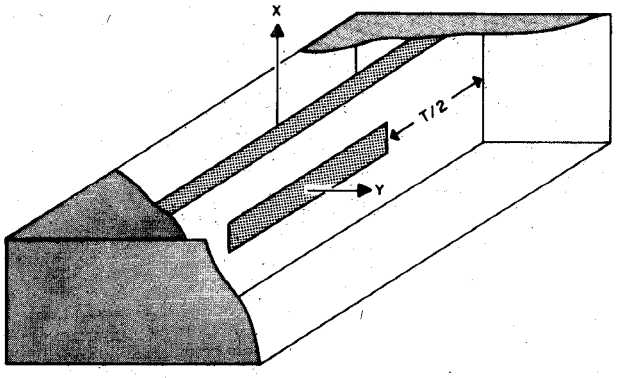

Fig. 4. View of a finline cavity terminated with inductive septae having half the length of the inductive strip between the coupled cavities shown in Fig. 1. The septae are backed by perfect electric walls.

where i and j range from 1 to Q and the E_{xi}^{z} and E_{xj}^{z} are sine functions for even index and cosine functions for odd index. The matrix represented by the bracketed term on the left in (6) is $Q \times Q$ and contains the elements of the inner product defined over α_n and ξ_k [5, eq. (11)].

Computationally, the first step is to determine the guide wavelength (see [3]) and then to find the odd- and even-mode resonant lengths of the two coupled cavities. The resonant lengths are found by computing the roots of the characteristic equation

$$\det\left[\langle\{E_x^x(\alpha_n)\}^2 G_{11} E_{xi}^z(\xi_k), E_{xj}^z(\xi_k)\rangle\right] = 0. \quad (7)$$

It should be noted that a single-term expansion leads to inaccurate results as discussed in [5].

A compromise must be made between numerical accuracy and computation time, which are both affected by the size of the search interval, limits of summation for the inner product, iteration accuracy (answer residue), and number of expansion terms used (order of the matrix). It was determined through convergence testing that a matrix of order 8 would permit odd- and even-mode resonant lengths to be computed with an accuracy of better than 2 percent when $W/b = 0.5$ or $W/b = 0.25$. For $W/b = 1$, a 12-term expansion of e_x was used.

Several limiting cases were investigated to check the correctness of the computer program. First, as the length T of the inductive strip increases to the point where the two cavities are uncoupled, the odd- and even-mode resonant lengths become equal. The end effect is the same as for a semi-infinite septum [5]. Second, as the length of the strip becomes infinitesimally small, the odd-mode resonant length approaches $\lambda'/2$. Lastly, consider a single cavity terminated at both ends by inductive septae having half the length of the strip coupling the two cavities and backed by perfect shorting walls as illustrated in Fig. 4. The resonant length of the odd mode of the coupled cavities is related to the resonant length of the single cavity by

$$l_0/\lambda' = l/\lambda' + l_{eq}/\lambda' \quad (8a)$$

where

$$l_{eq}/\lambda' = (1/2\pi)\tan^{-1}(x_{eq}) \quad (8b)$$

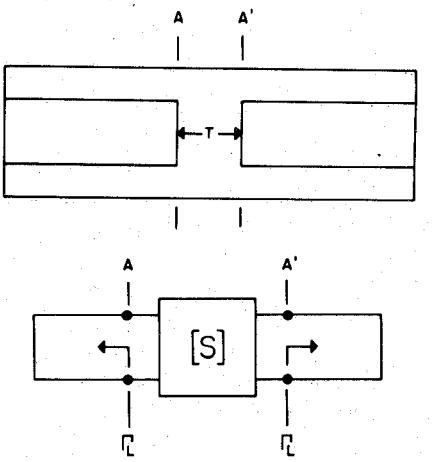

Fig. 5. Representation of the inductive strip by a two-port network characterized by the scattering matrix $[S]$.

and λ' is the guide wavelength. This last check is useful since the equivalent reactance x_{eq} of a variable length septum in a single cavity has been computed previously [5].

All these limiting cases were checked and the results were found to be correct to within 0.5 percent. This helped to develop confidence in the computer program.

The scattering coefficients of the inductive strip can be computed from the odd- and even-mode resonant lengths. To accomplish this, the strip is represented by a two-port network as depicted in Fig. 5. The inductive strip is lossless, reciprocal, and symmetric so its scattering matrix is unitary with $s_{12} = s_{21}$ and $s_{11} = s_{22}$. The unitary property leads to

$$|s_{21}| = \left[1 - |s_{11}|^2\right]^{1/2} \quad (9a)$$

$$\theta_{21} = \theta_{11} \pm \pi/2 \quad (9b)$$

where, in (9b), the minus $(-)$ sign is chosen because the strip is inductive. With reference to Fig. 5, Γ_L is the reflection coefficient looking into the perfectly shorted finline at the reference plane A or A' and may be written as

$$\Gamma_L = -1e^{-j2\beta l}. \quad (10)$$

Using (10), the scattering equations may be solved to find

$$s_{11} = \frac{1}{2}\left[\frac{\Gamma_{Le} + \Gamma_{Lo}}{\Gamma_{Le}\Gamma_{Lo}}\right] \quad (11a)$$

$$s_{21} = \frac{1}{2}\left[\frac{\Gamma_{Le} - \Gamma_{Lo}}{\Gamma_{Le}\Gamma_{Lo}}\right] \quad (11b)$$

where

$$\Gamma_{Le} = -e^{-j4\pi l_e/\lambda'} \quad (12a)$$

and

$$\Gamma_{Lo} = -e^{-j4\pi l_o/\lambda'}. \quad (12b)$$

From (11) and (12), we obtain the final result

$$s_{11} = \exp\left[j2\pi\left(l_e/\lambda' + l_o/\lambda'\right)\right]\cos 2\pi\left(l_e/\lambda' - l_o/\lambda'\right) \quad (13a)$$

$$s_{21} = j\exp\left[j2\pi\left(l_e/\lambda' + l_o/\lambda'\right)\right]\sin 2\pi\left(l_e/\lambda' - l_o/\lambda'\right). \quad (13b)$$

Throughout the above equations, the subscripts e and o denote the even and odd modes of the coupled cavities.

To summarize, the field equations are first solved to find the odd- and even-mode resonant lengths of the coupled finline cavities at a specified frequency. These lengths are then used to compute the scattering coefficients of the inductive strip coupling and cavities. It is evident from (13) that the magnitudes of the scattering coefficients depend upon the difference between the odd- and even-mode resonant lengths. It is therefore necessary to compute these lengths very accurately to obtain accurate values for the scattering coefficients. This implies that e_x must be expanded in a basis set that can approximate the true field distribution with a reasonable number of terms.

B. Experimental Method

The scattering coefficients of inductive strips in finlines have been measured in two ways. Direct measurements were made for strips etched from 2-mil-thick beryllium copper and centered in a WR (90) waveguide shield. The test fixture (shield) was 15 in long. For those cases where $W/b < 1.0$, the finline was matched to the WR (90) empty guide with a linearly tapered section. Except for the length, the test fixture, shorting blocks, and load are as described in [5] (see [5] for photographs). An HP 8409B Automatic Microwave Network Analyzer was used to measure $|s_{11}|$ and $|s_{21}|$ and θ_{11} was measured using a slotted line which seemed to produce better results.

Indirect measurement of strip scattering coefficients is also possible. In general, a reciprocal, symmetric two-port network is characterized by a scattering matrix which has four independent parameters: $|s_{11}|$, θ_{11}, $|s_{21}|$, and θ_{21}. Two identical strips can be used to form a high-Q finline resonator. It can be shown that the resonant frequency (f_0), Q, insertion loss (at f_0), and return loss (at f_0) are determined by the four independent parameters of the scattering matrix. If the strips (two-port networks) are lossless, then the situation is even simpler. The resonator properties are determined by $|s_{11}|$ and θ_{11} (see (9)). Conversely, the scattering coefficients (at f_0) may be expressed in terms of the resonator parameters. Measurement of the resonator response therefore permits the scattering coefficients to be computed. This approach has the advantage of requiring no phase information from the measurements. A scalar analyzer can be used. The approach is particularly attractive when it is difficult to establish reference planes for measurement of phase as it is when a strip is printed on a dielectric substrate. It is also a useful approach if a vector analyzer is unavailable, as is often the case at millimeter wavelengths. The disadvantage of this approach, of course, is that one resonator provides data for the computation of scattering coefficients at only a single frequency, f_0. Identical strips must be used to build resonators of several different lengths (different f_0's) to obtain values of scattering coefficients over a range of frequencies.

The derivation of the relations between resonator characteristics and strip scattering coefficients is lengthy. Therefore, a simpler and perhaps more satisfying approach will be used here. Numerical and experimental resonator insertion loss data will be presented and compared. Computed strip scattering coefficients have been used in the MICRO-Compact® program [8] to predict the resonator response numerically. The agreement between the predicted and measured response of the resonator is thus a good indication of the accuracy of the computed strip scattering coefficients. Since strips are used to build practical components such as filters, this type of comparison would ultimately be desired anyway and is therefore quite satisfying.

III. Numerical and Experimental Results

The spectral-domain analysis described in the previous section was implemented in a computer program, FINCAV. Numerical data generated using FINCAV were compared with experimental data to verify the accuracy of the computational results. To ease measurement difficulties, all measurements were made using X-band test structures. Shield size was 0.4 in $\times$ 0.9 in (WR (90)), and for those cases where no dielectric was present, the fins were centered in the shield. For $W/b < 1.0$, a linear taper was employed and where dielectric was present, a dielectric taper was used for matching purposes. Return loss for back to back tapers was measured and found to be greater than 20 dB. Direct measurement of scattering coefficients was accomplished using both a slotted line and an HP 8409B Automatic Vector Microwave Network Analyzer. In those cases where two inductive strips were used to form a resonator, the response was measured using an HP 8756 Scalar Network Analyzer with an HP 8350 Sweep Generator and plotter. Since a considerable amount of experimental data was collected, only representative results will be presented here.

A. Scattering Coefficient Measurements

Direct measurement of inductive strip scattering coefficients was made for several cases where no dielectric was present ($\epsilon_{r2} = 1$). With no dielectric, it is easy to establish the reference planes required for the measurement. Fig. 6 and 7 show $|s_{11}|$ and θ_{11} for several strips in finlines with $W/b = 1$. In the worst case, the difference between numerical and experimental data is about 7 percent. The rms error is much less. Similar data for $W/b = 0.25$ is shown in Figs. 8 and 9. The worst-case difference there is 5 percent. Data for s_{21} is not presented here since similar agreement was obtained. For lossless strips, s_{21} can be found from s_{11} using (9).

B. Resonator Measurements

A number of resonators were constructed using two identical inductive strips. Analysis shows that the resonant frequency is determined by

$$\theta_{11} = 2\pi l/\lambda' \tag{14}$$

where l is the distance between the strips. The shape of the transmission response curve over the band is determined by both $|s_{11}|$ and θ_{11}. As mentioned earlier, s_{11} completely defines the behavior of a lossless strip (see (9)). The reso-

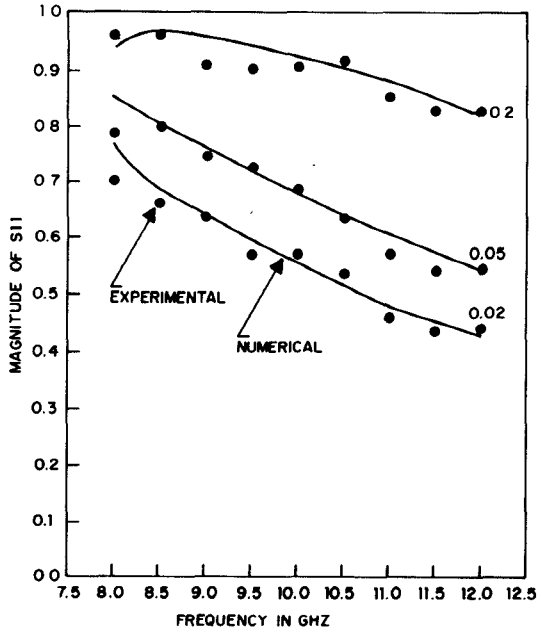

Fig. 6. $|s_{11}|$ versus frequency for $T = 0.02$-, 0.05-, and 0.2-in inductive strips centered in a WR (90) finline with $W/b = 1.0$ and $\epsilon_{r2} = 1.0$.

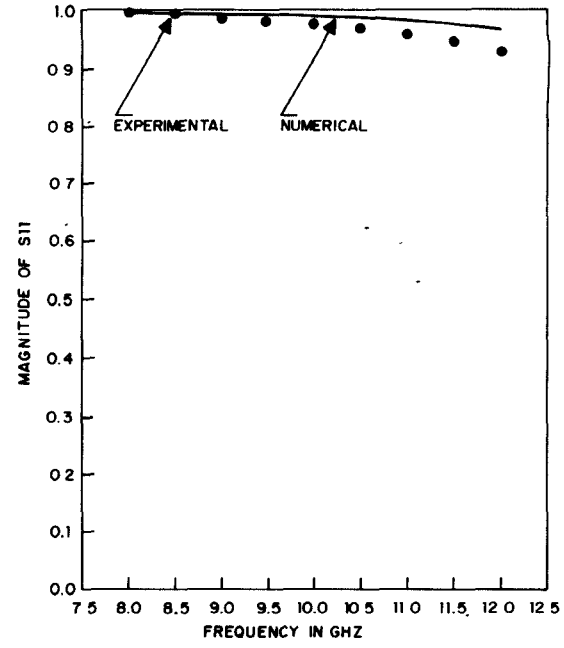

Fig. 8. $|s_{11}|$ versus frequency for a $T = 0.2$-in inductive strip centered in a WR (90) finline with $W/b = 0.25$ and $\epsilon_{r2} = 1.0$.

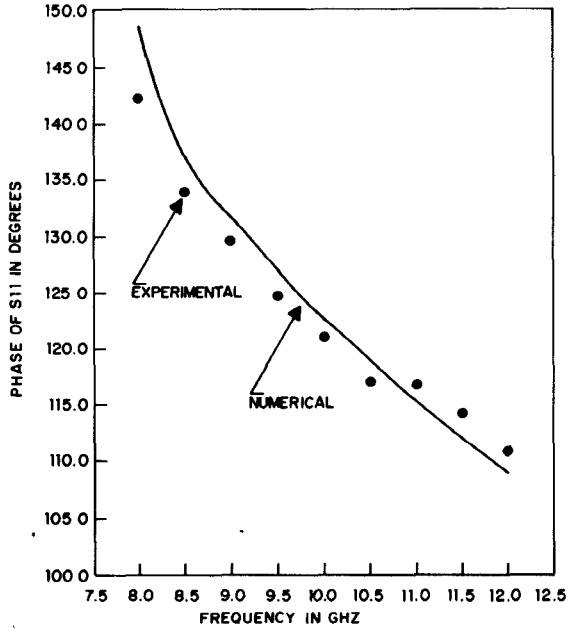

Fig. 7. θ_{11} versus frequency for $T = 0.05$-in inductive strip centered in a WR (90) finline with $W/b = 1.0$ and $\epsilon_{r2} = 1.0$.

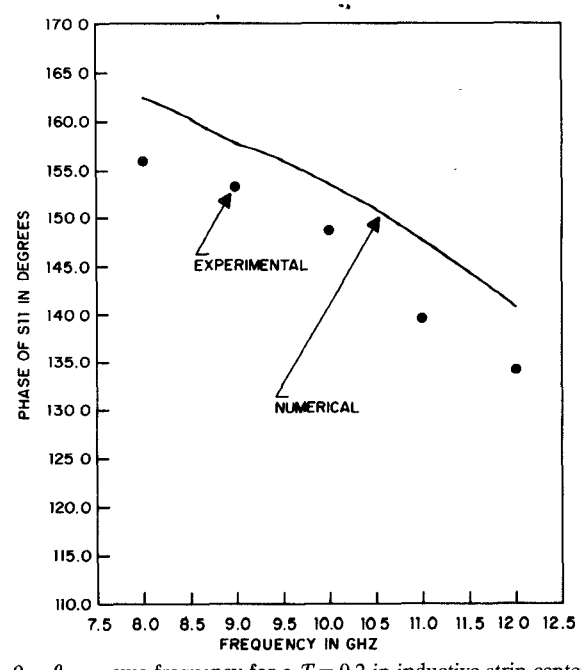

Fig. 9. θ_{11} versus frequency for a $T = 0.2$-in inductive strip centered in a WR (90) finline with $W/b = 0.25$ and $\epsilon_{r2} = 1.0$.

nator approach is particularly attractive when $\epsilon_{r2} > 1$ because it is difficult to establish reference planes for vector measurements.

The FINCAV program was used to compute scattering coefficients for the resonator inductive strips. The strips were modeled as two-port black boxes in MICRO-Compact®, and the computed values of the scattering coefficients were supplied as data for the 8–12-GHz band in 1-GHz steps. The resonator response predicted by MICRO-Compact® was compared with the measured response. Results for two resonators, one with dielectric and one without dielectric, will be presented here.

The first resonator had $W/b = 1.0$ and consisted of strips with length $T = 0.22$ in separated by a distance $l = 0.53$ in and centered in the WR (90) shield. The measured transmission response (solid curve) is shown in Fig. 10 along with the response predicted using MICRO-Compact® (circled points). The agreement is quite good. The predicted and measured resonant frequencies differed by only 0.5 percent (50 MHz) and the difference in the two transmission curves is only about 2 dB. The ripple in the measured response is due to the low VSWR coax-waveguide transitions which were used on each end of the finline test fixture.

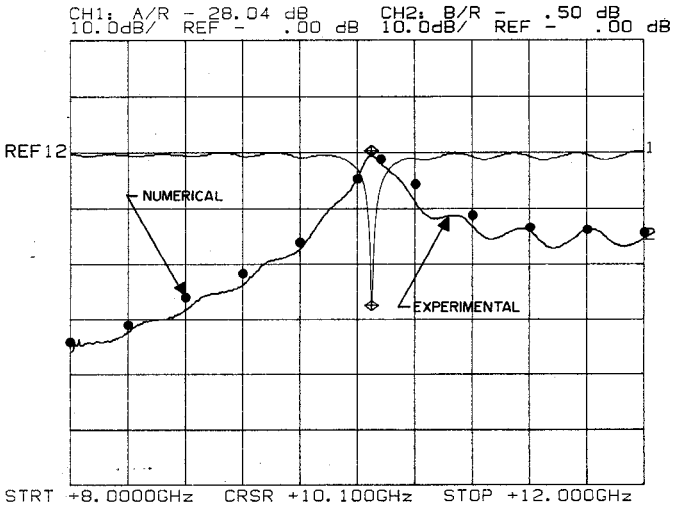

Fig. 10. Measured (solid curve) and predicted (circled points) transmission loss and return loss for a finline resonator. Inductive strips with $T = 0.22$ in are separated by 0.53 in and centered in the WR (90) shield with $\epsilon_{r2} = 1.0$.

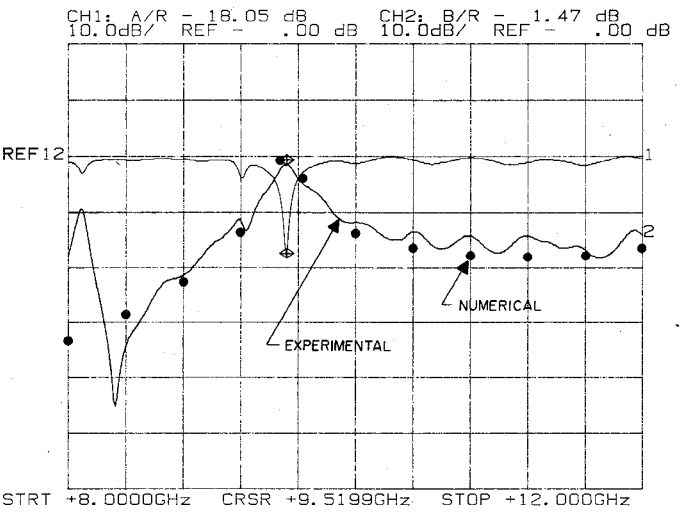

Fig. 11. Measured (solid curve) and predicted (circled points) transmission loss and return loss for a finline resonator. Inductive strips with $T = 0.22$ in are separated by 0.53 in and reside on a 1/32-in dielectric substrate with $\epsilon_{r2} = 2.5$, which is centered in the WR (90) shield.

The second resonator was identical to the first (within manufacturing tolerances) except the strips were printed on a 1/32 in dielectric substrate with $\epsilon_r = 2.5$. The substrate was centered in the WR (90) shield so the fins were 0.015-in off center. Slots extending through the shield walls were used to support the substrate, and the wall thickness was chosen equal to one quarter of a dielectric wavelength at band center, 10 GHz. Ideally, this causes an RF short circuit to appear at the inside wall but clearly represents a difference between the computer model and the actual test fixture. The measured transmission loss (solid curve) of this filter is shown in Fig. 11 along with the response predicted using MICRO-Compact® (circled points). The predicted and measured resonant frequencies differ by 0.2 percent (20 MHz). The difference between the measured and predicted response is generally 2–3 dB, although there are clearly several anomalies in the measured response below resonance. These were due to the slot which extended almost the full length of the 10-in test fixture. This suggests that the slots should not be any longer than necessary to support the dielectric substrate. It should be mentioned that the finline section between the two inductive strips in this resonator was also modeled as a two-port black box. Transmission phase data was derived from the computed finline dispersion. The overall response of this resonator is almost identical to that of the first resonator except that the resonant frequency is shifted down about 600 MHz (approx. 6 percent) by the presence of the dielectric substrate.

The agreement between predicted and measured resonator response was quite satisfying since strip scattering coefficients would most often be used in this manner.

C. *Errors*

Although good agreement between numerical and experimental data has been demonstrated, some discussion of the discrepancies is warranted. There are a number of sources of error which contribute to the differences seen in Figs. 6–11. Numerical computations were carried out with a goal of obtaining better than 2-percent accuracy for the values of odd- and even-mode resonant lengths. However, (13) shows that the scattering coefficients depend upon the difference, $(\lambda_e/\lambda' - \lambda_o/\lambda')$, so the s_{ij} may be in error by more than 2 percent. Another source of numerical error arises in the prediction of resonator response and is due to interpolation at frequencies between those for which scattering coefficient data were entered in the MICRO-Compact® program. Experimentally, there are a number of sources of error. Error in the determination of the reference plane for vector measurements and error due to transitions are discussed in [5]. Other sources of experimental error include losses, manufacturing tolerances, and instrumentation error (principally, sweeper frequency accuracy). Finally, when dielectric is used, any slot or groove used to support the substrate results in a physical structure which is different from the numerical model. These factors easily account for the observed differences between numerical and experimental data. Considerable effort would be required to further resolve the observed difference.

IV. Conclusions

This paper treats the general case of an inductive strip in a finline. The strip may be printed on a dielectric substrate and any value of $0 < W/b \leqslant 1.0$ is permitted. Previous papers have been restricted to special cases and have generally used other mathematical methods of analysis. This paper extends analysis to the most general case.

Numerical and experimental scattering coefficient data are presented for strips, and good agreement is demonstrated. The transmission response for several resonators has also been measured and compared with the predicted response based on use of the computed strip scattering

coefficients. Results agree within the limits imposed by the various sources of numerical and experimental error.

Lastly, the data presented here demonstrates the applicability of the spectral-domain technique to this discontinuity problem. This is particularly significant. Since the spectral-domain technique has previously been shown to work successfully for various configurations of strips and slots, the possibility exists that a single program could be created to analyze the behavior of various planar structures using this technique.

References

[1] P. J. Meier, "Integrated fin-line millimeter components," *IEEE Trans. Microwave Theory Tech.*, vol. MTT-22, pp. 1209–1216, Dec. 1974.

[2] K. Solbach, "The status of printed millimeter-wave *E*-plane circuits," *IEEE Trans. Microwave Theory Tech.*, vol. MTT-31, pp. 107–121, Feb. 1983.

[3] J. B. Knorr and P. M. Shayda, "Millimeter wave fin-line characteristics," *IEEE Trans. Microwave Theory Tech.*, vol. MTT-28, pp. 737–743, July 1980.

[4] R. H. Jansen, "Hybrid mode analysis of end effects of planar microwave and millimetrewave transmission lines," *Proc. Inst. Elec. Eng.*, vol. 128, pt. H, pp. 77–86, Apr. 1981.

[5] J. B. Knorr, "Equivalent reactance of a shorting septum in a finline: theory and experiment," *IEEE Trans. Microwave Theory Tech.*, vol. MTT-29, pp. 1196–1202, Nov. 1981.

[6] N. H. L. Koster and R. H. Jansen, "Some new results on the equivalent circuit parameters of the inductive strip discontinuity in unilateral fin-lines," *Arch. Elek. Übertragung.*, vol. 35, no. 12, pp. 497–499, 1981.

[7] R. H. Jansen and N. H. L. Koster, "A unified CAD basis for the frequency dependent characterization of strip, slot and coplanar MIC components," in *11th Eur. Microwave Conf. Proc.* (Amsterdam), 1981, pp. 682–687.

[8] MICRO-Compact®, available from Compact Software, 1131 San Antonio Road, Palo Alto, CA 94303.

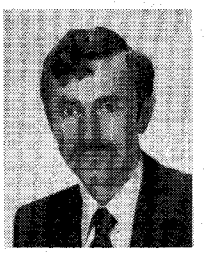

Jeffrey B. Knorr (S'68–M'71–SM'81) was born in Lincoln Park, NJ, on May 8, 1940. He received the B.S. and M.S. degrees in electrical engineering from Pennsylvania State University, University Park, PA, in 1963 and 1964, respectively, and the Ph.D. degree in electrical engineering from Cornell University, Ithaca, NY, in 1970.

From 1964 to 1967, he served with the U.S. Navy. In September 1970, he joined the faculty of the Naval Postgraduate School, Monterey, CA, where he currently holds the rank of Professor in the Department of Electrical Engineering and is the faculty director of the Microwave Laboratory. He is also a member of the Electronic Warfare Academic Group and the Space Systems Academic Advisory Committee. These groups are responsible for the administration of interdisciplinary programs in Electronic Warfare and Space Systems at the Naval Postgraduate School.

Dr. Knorr is a member of Sigma Xi and the Association of Old Crows.

✠

John C. Deal received the B.A. degree in physics from the University of Alaska, Fairbanks, AK, in 1973 and the M.S. degree in electrical engineering from the Naval Postgraduate School, Monterey, CA, in 1984. He joined the staff and faculty of the Department of Electrical Engineering at the United States Military Academy in 1984 and currently serves as an Assistant Professor. He has served in both tactical and strategic communications units as a primary staff officer and as a commander. Major Deal, an officer in the U.S. Army, Signal Corps, is a member of Eta Kappa Nu, Sigma Xi, and Phi Kappa Phi.